

A method for organs classification and fruit counting on pomegranate trees based on multi-features fusion and support vector machine by 3D point cloud

Chunlong Zhang, Kaifei Zhang, Luzhen Ge, Kunlin Zou, Song Wang, Junxiong Zhang*, Wei Li

College of Engineering, China Agricultural University, Haidian District, Beijing 100083, China



ARTICLE INFO

Keywords:
3D point cloud
Organs classification
Horticulture work
Multi-features fusion
Support vector machine

ABSTRACT

Organs classification and fruit counting on pomegranate trees are of great significance for horticulture works and robotic picking. However, there are still some challenges: (1) illumination is uncontrollable in the natural environment; (2) traditional 2D image-based methods for classification and recognition are limited by occlusion on pomegranate trees. In this paper, a method for organs classification and fruit counting on pomegranate trees based on multi-features fusion and Support Vector Machine (SVM) was proposed. It was constructed by the following steps: (1) Three-dimensional point clouds of pomegranate trees were obtained by an RGB-D camera; (2) Three-dimensional point clouds were preprocessed; (3) Color and shape features were extracted to train the SVM classifier; (4) The obtained classifier model was used for organs classification on pomegranate trees; (5) A K-nearest neighbor (KNN) smoothing based on weighted Euclidean distance was used to improve the accuracy of classification; (6) An agglomerative-divisive hierarchical clustering was used to count pomegranate fruit. The experiment results showed that the SVM classifier based on color and shape feature had an accuracy of 0.75 for fruit and 0.99 for non-fruit. The fruit counting based on agglomerative-divisive hierarchical clustering had a recall of 87.74 % and a precision of 78.15 %. Compared with density-based spatial clustering of applications with noise (DBSCAN), the recall has improved significantly. This method was aimed at the whole fruit tree, so it has advantages in the completeness of information. The results indicated that the proposed method was effective and feasible for organs classification and yield estimation on pomegranate trees in the natural environment.

1. Introduction

Organs classification and fruit counting are important for horticulture works in orchard management. Recognition and counting of fruit can be used to identify the growing stage and estimate yield. Spatial localization of fruit can be used to guide robotic picking. The identification of leaf can be used for precision spraying (Westling et al., 2018). Trunk and branch recognition can be used for the pruning, which affects the quantity and quality of fruit (Rosell et al., 2012). In recent years, many researchers have researched organs classification and recognition on fruit trees.

Some researchers have researched the fruit recognition methods based on 2D image (such as colors, shapes and textures). These methods have achieved good results. In these works, different color spaces (such as RGB, YCbCr and YUV) were used to extract different color features (Mohammadi et al., 2015; Lei et al., 2019; Liu et al., 2019a,b; Li et al.,

2018). Shape descriptors were used to extract shape features, such as histogram of oriented gradient (HOG) (Liu et al., 2019a,b), Hough transformation and shape context algorithm (Gongal et al., 2016; Lu et al., 2018; Linker, 2017; Niu, 2017). Lv et al. (2019a, b) proposed a method based on control limited adaptive histogram equalization (CLAHE) algorithm for bagged green apple image segmentation. In some works, template matching with weighted Euclidean distance (TMWE) (Tan et al., 2018), weighted relevance vector machine (RVM) (Wu et al., 2019), classification and regression tree classifier (Yamamoto et al., 2014), etc. were used to identify fruit. Recently, methods for fruit recognition based on deep learning have been used in researchers' works, such as convolutional neural network (CNN) (Bargoti et al., 2017), pulse coupled neural network (PCNN) (Xu et al., 2018) and faster regions with CNN features (faster RCNN) (Stein et al., 2016). However, deep learning requires a lot of data and takes a lot of time to train models. Fruit counting is an important part of yield estimation.

* Corresponding author.

E-mail address: zhang_junxiong@163.com (J. Zhang).

Researchers mostly counted fruit by clustering. Such as X-means (Yamamoto et al., 2014), clustering algorithm based on Euclidian distance (Gongal et al., 2016), kernel fuzzy C-means (Lei et al., 2019). In addition, thermal images (Gan et al., 2018) was used to identify fruit. In Lv et al., 2019a, b, a apple image segmentation method based on convex hull center priori and Markov adsorption chain was proposed with a ultimate measurement accuracy of 3.15 % and a IoU of 95.65 %. In summary, although features (such as color, shape, texture) by 2D image were used for fruit recognition and organs classification, there were still some challenges: (1) Shape features extracted from 2D images were incomplete, and then, (2) fruit by 2D images were occluded, which was an important factor affecting fruit recognition and organs classification in horticulture works.

Compared with 2D images, 3D point clouds shows more complete plant information. There are three methods for acquiring 3D point cloud: (1) Large-scale, high-precision and high-cost equipment, such as 3D laser scanners (Pearse et al., 2019; Calders et al., 2015; Yang et al., 2018; Jamayet et al., 2018; Park et al., 2018), laser radar (Madec et al., 2017; Yan et al., 2015; Li et al., 2019; Krishna et al., 2019; Qiu et al., 2019), and ultrasonic (Hu et al., 2018; Gangadharan et al., 2019). These devices are generally used for three-dimensional reconstruction of large-scale scenes, such as forest reconstruction, building large-scale three-dimensional maps, etc., and have high accuracy in the reconstruction of large-scale scenes. However, they are expensive, so their application in general scene reconstruction is limited. (2) Small-range, moderate-precision and low-cost RGB-D camera (Wang et al., 2017; Chiu et al., 2019; Tu et al., 2018; Gené-Mola et al., 2019). Depth cameras are generally used for 3D reconstruction of small scenes, such as indoor scene reconstruction, human body 3D reconstruction, etc. They generally have a shooting range not more than ten meters, and has high accuracy in small-scale scene reconstruction. (3) Reconstruct 3D point cloud based on multiple images (Dey et al., 2012; Zhou et al., 2019; Jay et al., 2015). This method can directly use the ordinary camera to obtain the two-dimensional image of the scene, but its reconstruction accuracy is affected by the algorithm and the resolution of the camera. In recent years, the SVM classifiers based on color and 3D shape features have been commonly used by researchers (Dey et al., 2012; Tao et al., 2017; Avendano et al., 2017; Ramos et al., 2018). A method based on color-fast point feature histogram (Color-FPFH) descriptors and SVM classifier for organs classification and fruit recognition on apple trees was proposed in Tao et al. (2017). Some researchers identified fruit by only 3D features. A method based on convex template Instance (CTI) descriptor for various fruit (such as tomato, apple) recognition was proposed in Nyarko et al. (2018). In addition, clustering was used by researchers to detect individual fruit. In Díaz et al. (2018), an approach based on density-based spatial clustering of applications with noise (DBSCAN) for grape buds detection in winter was proposed with a precision of 100 % and a recall of 45 %. In Lin et al. (2019), a method for guava segmentation based on Euclidean clustering was proposed with a precision of 98.3 % and a recall of 94.8 %. In summary, the 3D point cloud shows more complete shape features of fruit trees than the 2D image, and has some improvement on occlusion condition, therefore, the 3D point cloud is better to identify fruit and classify organs in horticulture works.

In this paper, a method for organs classification and fruit counting on pomegranate trees was proposed. This method uses the fusion of the shape and color features of the three-dimensional point cloud to classify organs. Previously, the shape descriptor (Kleppe et al., 2018) were mostly used for identification and detection of industrial robots, and their applications in agriculture were few. The proposed method can be used for various operations such as pruning, spraying and yield estimation in orchards in the natural environment.

2. Materials and methods

2.1. Data acquisition of pomegranate trees

In this paper, the 3D point cloud data of pomegranate trees obtained by the RGB-D camera (RealSense D435, Intel, California, USA) was acquired in China Agricultural University (116°20'59"E, 40°0'19"N) from July 20, 2019 to August 26, 2019. Three-dimensional point clouds of six pomegranate trees were reconstructed, and they were all in the mature stage. The support software was Dot3D (Dot Product), and the algorithm ran on MatlabR2019a (MathWorks, Massachusetts, USA). The work platform was a PC equipped with Windows 10, 64-bit system (DirectX 12), 16 GB RAM, Intel Core i7-8750 @ 2.20 GHz.

2.2. Organs classification and fruit counting processing pipeline

2.2.1. Three dimension point clouds preprocessing

The 3D point cloud of pomegranate trees obtained in the natural environment was complicated, so it was difficult to be classified. In order to improve the quality of point cloud, the point cloud was pre-processed before classification. In this paper, the point cloud pre-processing was divided into three steps: (1) background removed; (2) down sampling based on voxel grid filter (Pomerleau et al., 2013) with a uniform step size (8 mm); and (3) outlier filtering (Fig. 1).

Firstly, the background in original 3D point cloud was removed manually by Meshlab software. Secondly, the 3D point cloud was down sampled based on the voxel grid filter with a uniform step size (8 mm). Finally, outlier filtering was used to remove outliers in the point cloud.

2.2.2. Color and shape features extraction

In this paper, color and shape features were used to train the SVM classifier. The color features included red, green and blue channels. Then, a shape descriptor (Kleppe et al., 2018) was used for shape features extraction. Fruit, branch, and leaf in 3D point cloud were considered as 'sphere', 'cylinder', and 'flat', because they have different shape features. As shown in Fig. 2.

In the 3D point cloud, k-dimensional tree was built to index neighborhood points for each point. Next, covariance matrix was established by the coordinates of neighborhood points, as in Eq. (1). Then three eigenvalues of covariance matrix were calculated. Finally, the shape features were showed by Eqs. (2)–(4).

$$c = \begin{pmatrix} \text{cov}(x,x) & \text{cov}(x,y) & \text{cov}(x,z) \\ \text{cov}(y,x) & \text{cov}(y,y) & \text{cov}(y,z) \\ \text{cov}(z,x) & \text{cov}(z,y) & \text{cov}(z,z) \end{pmatrix} \quad (1)$$

Where x, y, z denotes three coordinates of neighborhood points, respectively.

$$\epsilon_1 = \frac{d_1 - d_2}{d_1 + d_2 + d_3} \quad (2)$$

$$\epsilon_2 = \frac{2 \times (d_2 - d_3)}{d_1 + d_2 + d_3} \quad (3)$$

$$\epsilon_3 = \frac{3 \times d_3}{d_1 + d_2 + d_3} \quad (4)$$

Where d_1, d_2, d_3 respectively denotes three eigenvalues of covariance matrix, and $\epsilon_1, \epsilon_2, \epsilon_3$ denotes three shape descriptors, respectively.

Limited by scales of three categories, this method had different performances by different scales of neighborhoods. Therefore, in order to improve the accuracy of organs classification, three different scales of neighborhoods ($k_1 = 200$, $k_2 = 400$, $k_3 = 800$) were used to classify each point in point cloud of pomegranate trees. Where k_1, k_2 and k_3 refer to the thresholds when searching for neighborhoods. For example, the ' $k_1 = 200$ ' means the number of neighborhood points is 200.

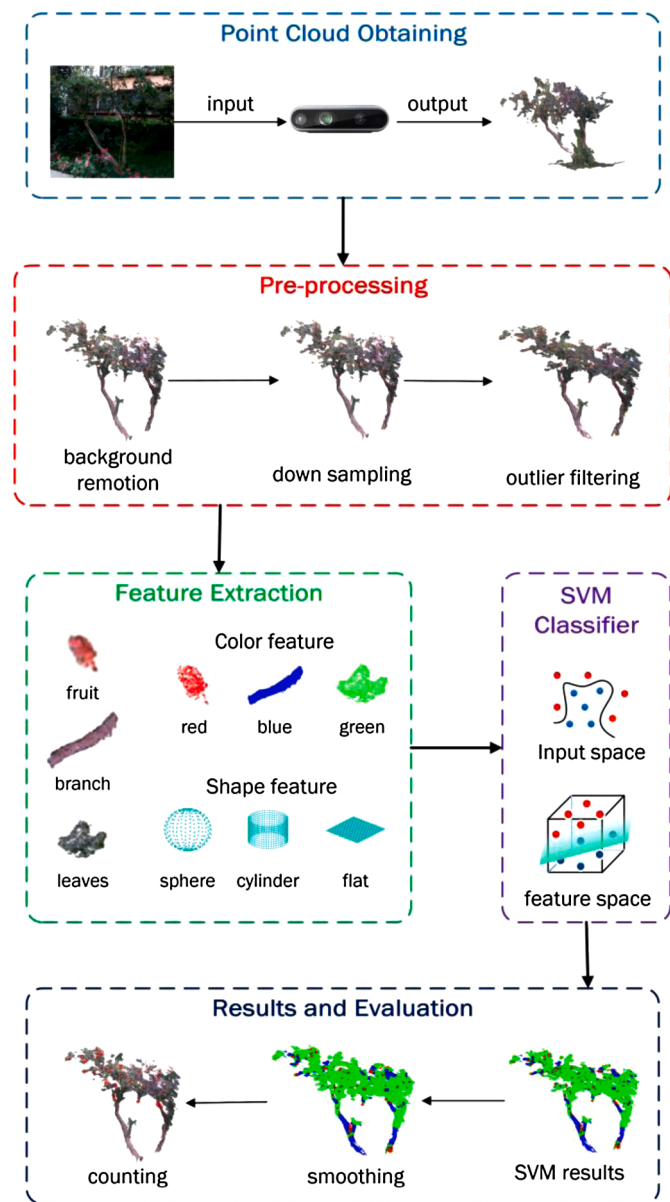


Fig. 1. Organs classification and fruit counting processing pipeline.

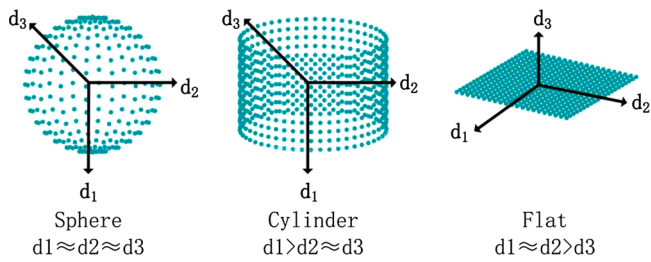


Fig. 2. Shape features of sphere, cylinder and flat.

2.2.3. Organs classification of pomegranate trees

In this paper, the SVM classifier was used for organs classification. Support vector machine classifier is stable, with a variety of different kernel functions to choose from. As for other machine learning methods, such as neural networks require a large amount of data and parameters, and has poor interpretability. As another example, the random forest algorithm is prone to overfitting when the sample noise in this paper is

large. The libsvm 3.2.3 (Lin et al., 2011) with radial basis function (RBF) was used to construct models. The radial basis function is suitable for the multi-classification problem in this paper, and it is less sensitive to noise.

The data set (point cloud with 961,003 points) used for training SVM classifier was manually divided into three categories: fruit, branch and leaf. Color features (R, G, B) and shape features (three-scale neighborhoods) were combined to form a 12-dimensional feature vector. Then a part of the point cloud (159,613 points) was used as a training set to train an SVM classifier with an RBF kernel, and remaining point cloud (801,390 points) was used as a testing set. Finally, the SVM classifier with feature vectors as input was used for organs classification.

2.2.4. KNN smoothing based on weighted Euclidean distance

In 3D point cloud, each point was given a separate label by SVM classifier, therefore, the classification results of the SVM classifier were noisy. In a neighborhood, the similarity between points was related to the distance between them, so the KNN smoothing based on weighted Euclidean distance was used to smooth the results of the SVM classifier, as shown in Eq. (5). In contrast, for other methods, such as histogram points using neighbors for equalization, there was no weight value, so its priority was lower.

$$p = \frac{\sum_{i=1}^k ((k+1-i) \times p_i)}{\sum_{i=1}^k i} \quad (5)$$

Where p denotes a point of point cloud, and p_i denotes k neighbors of point p .

In 3D point cloud, the KNN smoothing based on weighted Euclidean distance was used to correct the label of point p . The weight value depends on distance between point p and its neighborhood point. Finally, the label of point p was consistent with its neighborhood points.

The appropriate scale of neighborhood was important in the smoothing of organs classification. In this paper, the neighborhood with a scale ($k = 50$) was used for the smoothing of organs classification.

2.2.5. Fruit counting based on agglomerative-divisive hierarchical clustering

The accuracy of counting was important to yield estimation. The agglomerative-divisive hierarchical clustering was used for fruit counting. Firstly, the agglomerative hierarchical clustering based on Euclidean distance threshold was used to aggregate independent points into different clusters. The threshold depended on number of points in clusters. The divisive hierarchical clustering was used to divide clusters with the number of points exceeding the threshold in smaller clusters. In this paper, a separate agglomerative hierarchical clustering was used to compare with the agglomerative-divisive hierarchical clustering in order to reflect the effectiveness of the latter.

2.2.6. Methods of evaluation

In this paper, Precision-Recall curve (PR curve) was used to evaluate the overall performance of SVM classifier. Recall and precision were as shown in Eqs. (6) and (7).

$$\text{precision} = \frac{TP}{TP + FP} \quad (6)$$

$$\text{recall} = \frac{TP}{TP + FN} \quad (7)$$

Where TP denotes the number of true positives, TN denotes the number of true negatives, FP denotes the number of false positives, and FN denotes the number of false negatives.

The PR curve can show the overall performance of SVM classifier. When a curve completely embraces another curve, the former is considered to have a better performance. When two curves intersect, the performances of curves was evaluated by area under curve (AUC).

Recall, precision and F1-score were used to evaluate fruit counting of pomegranate trees. As shown in Eqs. (6)–(8).

$$F1\text{-}score = \frac{2 \times recall \times precision}{recall + precision} \quad (8)$$

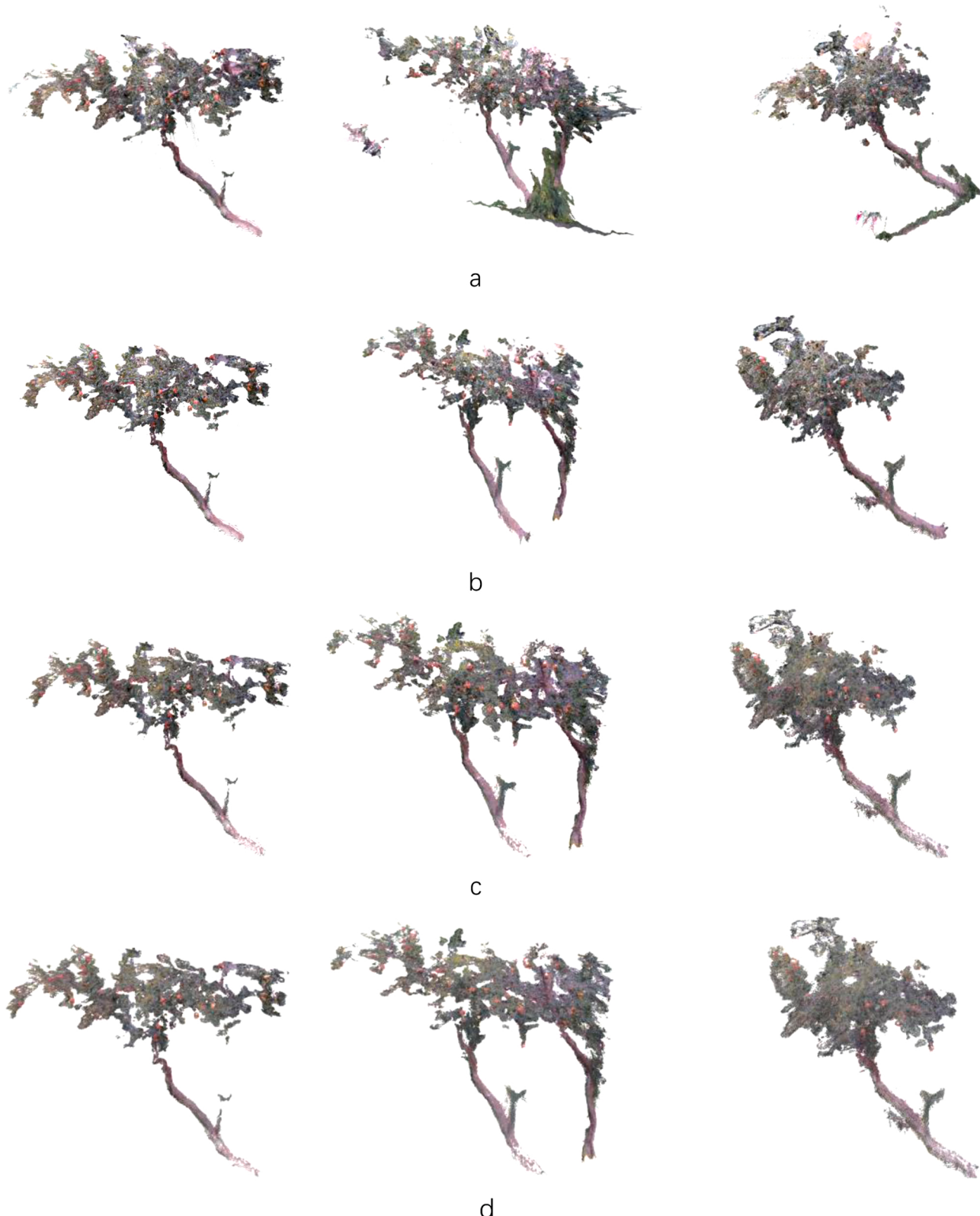


Fig. 3. The 3D point cloud preprocessing. (a) Original 3D point cloud. (b) Results of background removed. (c) Results of down sampling. (d) Results of outlier filtering.

3. Results and discussion

3.1. Point cloud preprocessing

The preprocessing of 3D point cloud was shown in Fig. 3. The original point cloud (13,244,046 points) obtained by RGB-D camera was shown in Fig. 3a. The background of original point cloud was removed in Fig. 3b, and the number of points was reduced to 7116143. The results of down sampling was shown in Fig. 3c. The point cloud after preprocessing for a total of 961,003 points. The result of outlier filtering was shown in Fig. 3d.

3.2. Organs classification

The results of organs classification by the SVM classifier was shown in Fig. 4a. The PR curve of organs classification with different dimensional feature vectors was shown in Fig. 5. The AUC values of PR curves

of different organs was shown in Table 1. In these figures, curves based on color with 2-scale shape ($k_1 = 200$, $k_2 = 400$) outperform other curves in all categories. As a result, the SVM classifier got an AUC of 0.75307 for fruit, an AUC of 0.99701 for non-fruit, an AUC of 0.34601 for branch and an AUC of 0.97985 for leaf. In summary, the SVM classifier had better performance for fruit and non-fruit than for fruit, leaf and branch. In the process of organs classification, color features were affected by the illumination and fruit growing stage. Therefore, the organs classification with only color features was unstable, while the organs classification with color and shape features was not sensitive to illumination. For shape features, the neighborhood with a small scale suitable for extracting shape features of fruit and leaf, while the neighborhood with a large scale suitable for extracting shape features of branch.

Compared with the color-FPFH (Tao et al., 2017) method, the method proposed in this paper has a higher classification accuracy for leaf and a lower classification accuracy for fruit and branch, which has

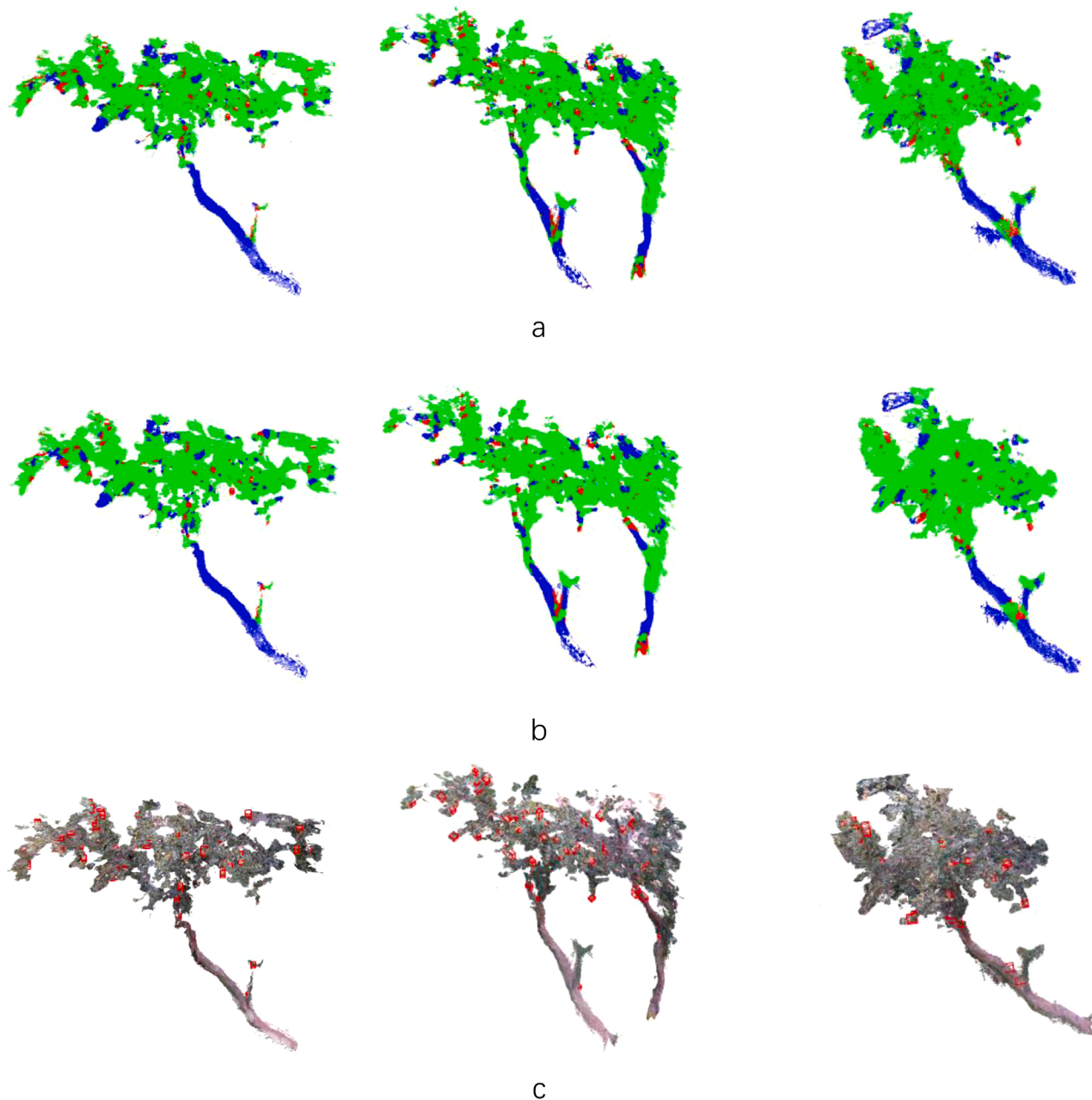


Fig. 4. Organs classification and fruit counting of 3D point cloud. (a) Results of organs classification. (b) Results of smoothing. (c) Results of fruit counting.

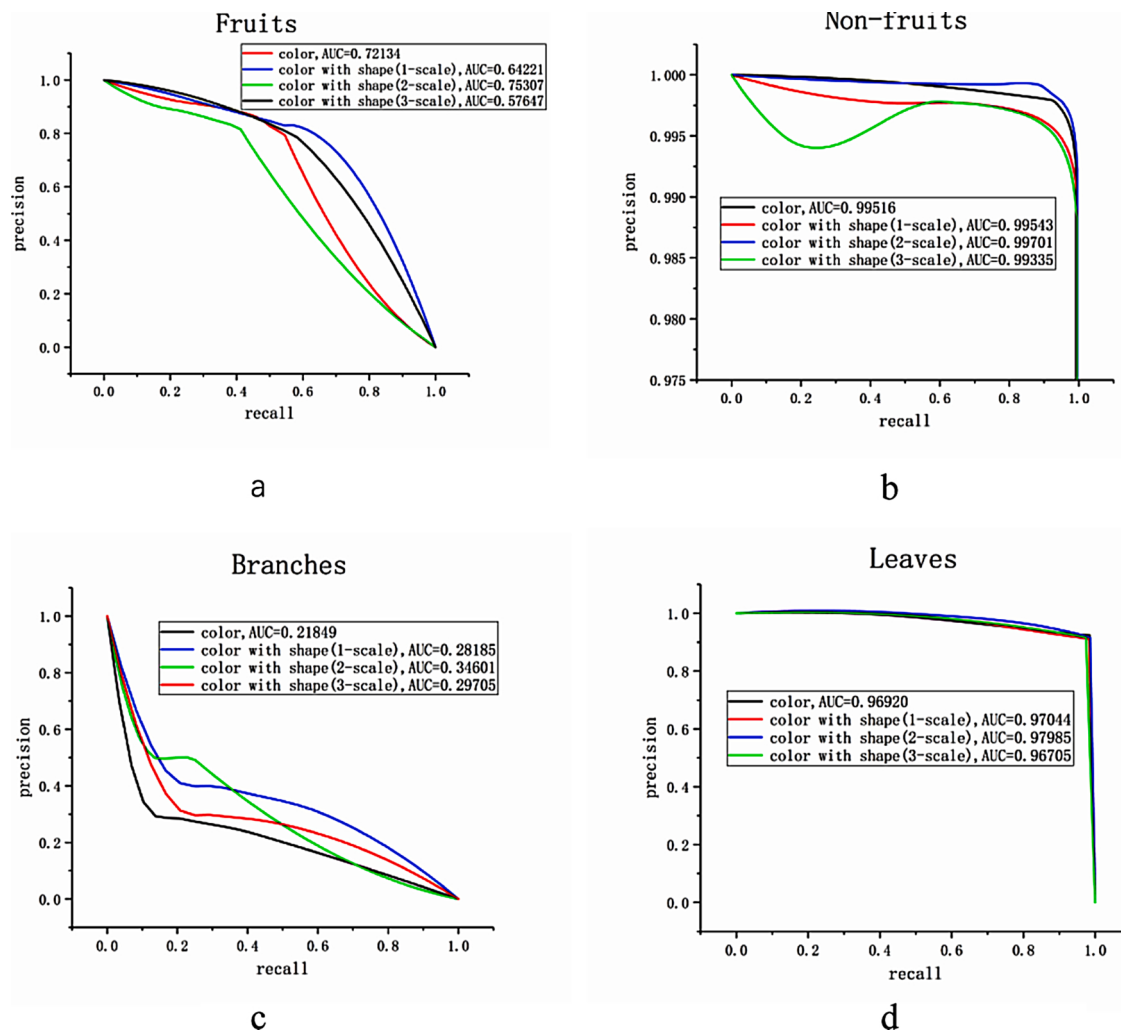


Fig. 5. PR curves obtained by SVM classifier. (a) Fruit. (b) Non-fruit. (c) Branch. (d) Leaf.

Table 1

The AUC values of PR curves of fruit, branch and leaf.

organs	AUC			
	color	Shape(1-scale) with color	Shape(2-scale) with color	Shape(3-scale) with color
fruit	0.72134	0.64221	0.75307	0.57647
branch	0.21849	0.28185	0.34601	0.29705
leaf	0.96920	0.97044	0.97985	0.96705
non-fruit	0.99516	0.99543	0.99701	0.99335

some influences. First, the samples used were more complicated. Secondly, their method was oriented towards a part of the fruit tree, and the object of our method was the whole fruit tree, which increased the difficulty of classification. The method proposed needs to be further improved, especially in the classification for branches. The result of organs classification on branch was not good due to the difference in the number of points on branch and non-branch and the poor color features of branch. The result of classification on branch with only shape features was not good. The poor color features resulted in the misclassification on branch, and the difference in the number of points on branch and non-branch resulted in the low accuracy of branch. The results of classification were affected by color and shape features. For color features, the similar color features between branch and some of fruit resulted in misclassification. For shape features, the similar size between leaf and

some of fruit resulted in misclassification in shape features.

3.3. The KNN smoothing based on weighted Euclidean distance

The performance of KNN smoothing was shown in Figs. 6 and 4 b. As shown in these figures, noises caused by the SVM classifier were removed by this method. For this smoothing, the scale of neighborhood was important due to the difference in size and occlusion of fruit. The neighborhood with a large scale resulted in a loss of occluded fruit or small fruit, while the neighborhood with a small scale resulted in a not significant smoothing. In this paper, the scale of neighborhood was chosen as: $k = 50$.

The performance of fruit counting before and after smoothing was shown in Table 2. In this method, the KNN smoothing based on weighted Euclidean distance was used to smooth the results of SVM classifier, because the label of a point was affected by the label of its neighborhood points. The number of neighborhood points was compared with 20, 50 and 100. It could be seen from the Table 2 that the smoothing effect was the best when $k = 50$. The number of positive increased from 85 to 93 before and after smoothing, and the number of negative reduced from 35 to 26. Recall, precision and F1-score of fruit counting increased from 80.19 %, 70.83 % and 75.23 %–87.74 %, 78.15 % and 82.67 % before and after smoothing. When $k = 20$, the smoothing effect was not significant, because the number of neighborhood points was too small. When $k = 100$, the number of neighborhood points was so large that there was too much noise, which reduced the smoothing effect. In

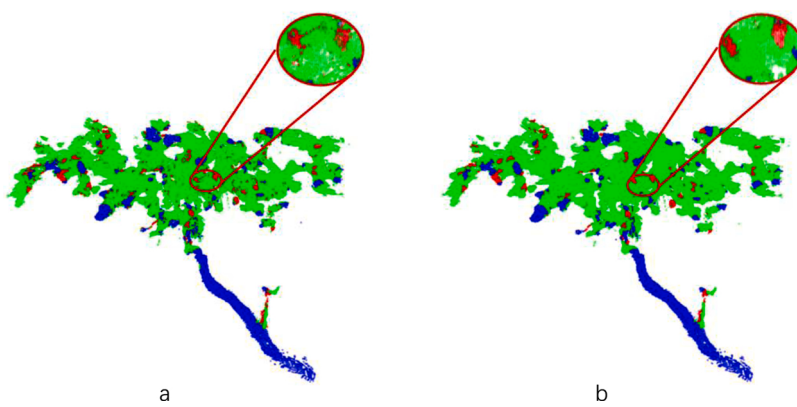


Fig. 6. Comparison before and after smoothing. (a) Classification result before smoothing. (b) Classification result after smoothing.

Table 2

The results of fruit counting before and after smoothing.

Counting	Fruit	Positive	Negative	Recall (%)	Precision (%)	F1-score (%)
Before smoothing	106	85	35	80.19	70.83	75.23
After smoothing ($k = 20$)	106	87	33	82.08	72.50	76.99
After smoothing ($k = 50$)	106	93	26	87.74	78.15	82.67
After smoothing ($k = 100$)	106	90	31	84.91	74.38	79.30

summary, the results of SVM classifier were improved effectively by the KNN smoothing based on weighted Euclidean distance.

3.4. Fruit counting based on agglomerative-divisive hierarchical clustering

The results of agglomerative-divisive hierarchical clustering and individual agglomerative hierarchical clustering on fruit counting were shown in Table 3. In the process of fruit counting, the individual agglomerative hierarchical clustering only cluster points by a 'bottom-up' manner, and it results in some large clusters with multiple fruit or non-fruit. While the agglomerative-divisive hierarchical clustering cluster points by a 'bottom-up-bottom' manner, and it divides large clusters into small clusters. As a result, the fruit counting got a recall of 80.19 %, a precision of 68.55 %, an F1-score of 73.91 % by individual agglomerative hierarchical clustering and a recall of 87.74 %, a precision of 78.15 %, an F1-score of 82.67 % by agglomerative-divisive hierarchical clustering. In summary, the agglomerative-divisive hierarchical clustering outperformed the individual agglomerative hierarchical clustering in this paper.

In Díaz et al. (2018), an approach based on DBSCAN for grape buds detection in winter was proposed with a precision of 100 % and a recall of 45 %. Compared with their method, the method proposed had a precision of 78.15 % and a recall of 87.74 %. Our precision was lower, but the recall had improved significantly. This was because DBSCAN can only determine the attribution of points by a single threshold, while our method adjusts by double thresholds.

Table 3

Comparison of the results obtained in agglomerative hierarchical clustering and agglomerative-divisive hierarchical clustering.

Counting	Fruit	Positive	Negative	Recall (%)	Precision (%)	F1-score (%)
agglomerative hierarchical clustering	106	85	39	80.19	68.55	73.91
agglomerative-divisive hierarchical clustering	106	93	26	87.74	78.15	82.67

The point clouds after fruit counting were shown in Figs. 7 and 4 c. Where the 3D point cloud of pomegranate tree was shown in Figs. 7a and 4 c. In Fig. 7b, fruit in the point cloud were marked by 3D boxes. The point cloud of fruit detected was shown in Fig. 7c. The fruit at the same angle with Fig. 7b were shown in Fig. 7d. These figures show most of fruit were marked by 3D boxes. Errors of fruit counting were affected by color and shape features. For color features, the similar color features between branch and some of fruit resulted in errors of color features extracted. For shape features, the similar size between leaf and some of fruit resulted in errors of shape features extracted.

4. Conclusion

In this paper, the 3D point clouds of pomegranate trees were obtained by RGB-D camera, and they were preprocessed. Then three channels of RGB space were combined with shape features. Then the SVM classifier with color and 2-scale shape ($k_1 = 200$, $k_2 = 400$) features was used for organs classification on pomegranate trees and got an AUC of 0.75307 for fruit, an AUC of 0.99701 for non-fruit, an AUC of 0.34601 for branch, an AUC of 0.97985 for leaf. Next, The KNN ($k = 50$) smoothing based on weighted Euclidean distance was used to improve the accuracy of organs classification and fruit counting. This method resulted in a recall of 87.74 %, a precision of 78.15 % and an F1-score of 82.67 % for fruit counting. Finally, The agglomerative-divisive hierarchical clustering increased recall of 7.55 % compared with the agglomerative hierarchical clustering, and got a recall of 87.74 % for fruit counting. This indicated that this method can detect most of fruit on trees.

The traditional two-dimensional image-based methods only recognize one side of the fruit tree, and the existing three-dimensional point cloud-based methods mostly target part of the fruit tree. In contrast, the method proposed classifies and recognizes the whole fruit tree. Although the recognition effect of some organs were lower, it has advantages in the completeness of information. This method can be used to provide a reference for horticulture works and robotic picking in the natural environment. In future research, we will challenge to get 3D point clouds with a higher accuracy for horticulture works.

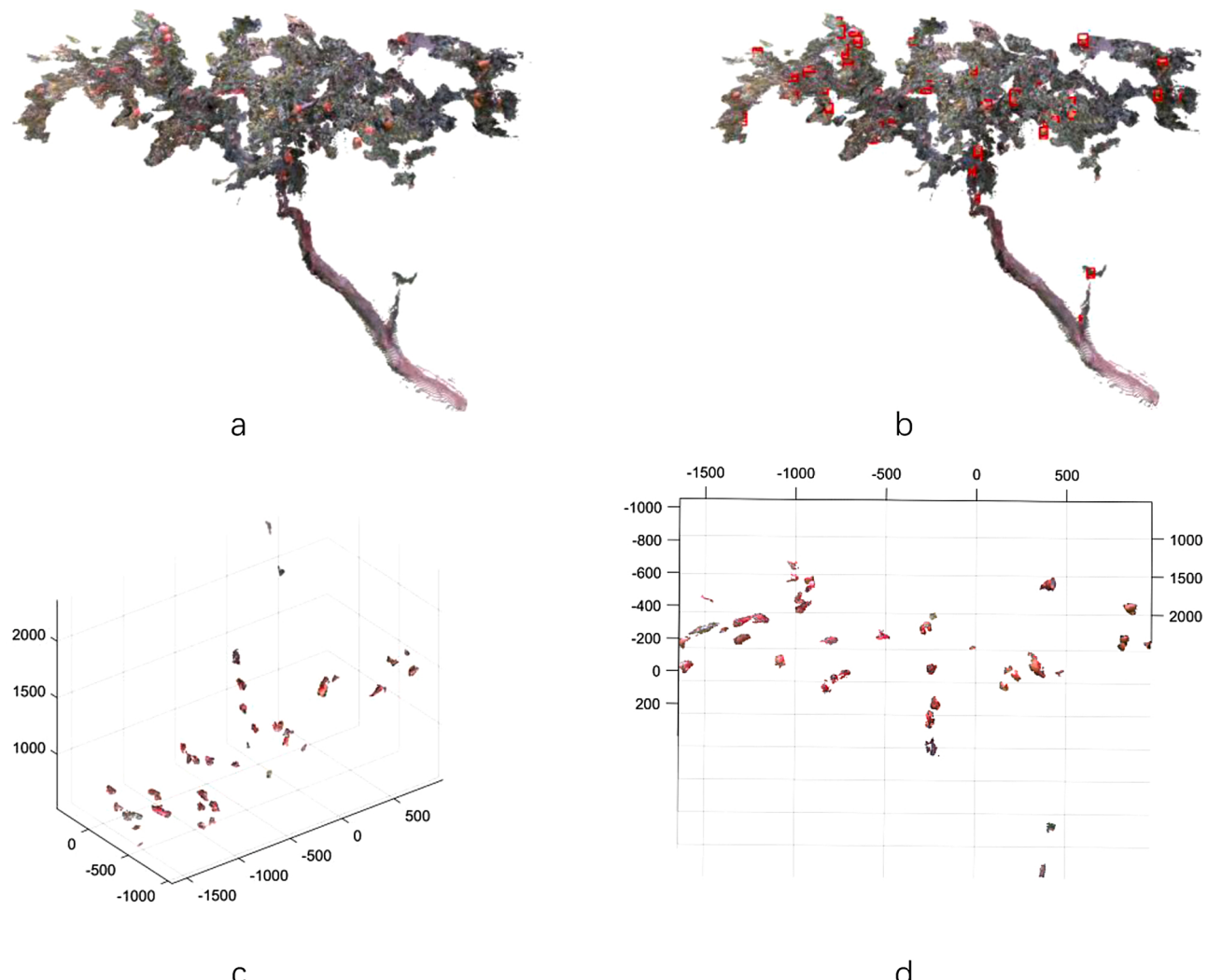


Fig. 7. Results of fruit counting. (a) Original point cloud. (b) Fruit were marked with 3D box. (c) Fruit were extracted from the point cloud. (d) Fruit at the same angle.

Author contributions

Conceptualization, Chunlong Zhang; Data curation, Chunlong Zhang and Kaifei Zhang; Funding acquisition, Junxiong Zhang; Methodology, Chunlong Zhang; Project administration, Junxiong Zhang; Software, Kaifei Zhang; Writing – original draft, Chunlong Zhang; Writing – review & editing, Kaifei Zhang, Luzhen Ge, Kunlin Zou, Song Wang, Junxiong Zhang and Wei Li

Funding

This work was supported by National Natural Science Foundation of China (31601217).

CRediT authorship contribution statement

Chunlong Zhang: Conceptualization, Data curation, Methodology, Writing - original draft. **Kaifei Zhang:** Data curation, Software, Writing - review & editing. **Luzhen Ge:** Writing - review & editing. **Kunlin Zou:** Writing - review & editing. **Song Wang:** Writing - review & editing. **Junxiong Zhang:** Funding acquisition, Project administration, Writing - review & editing. **Wei Li:** Writing - review & editing.

Declaration of Competing Interest

The authors declare that they have no known competing financial interests or personal relationships that could have appeared to influence the work reported in this paper.

References

- Avendano, J., Ramos, P.J., Prieto, F.A., 2017. A system for classifying vegetative structures on coffee branch based on videos recorded in the field by a mobile device. *Expert Syst. Appl.* 88, 178–192.
- Bargoti, S., Underwood, J.P., 2017. Image segmentation for fruit detection and yield estimation in apple orchards. *J. Field Robot.* 34 (6), 1039–1060.
- Calders, K., et al., 2015. Nondestructive estimates of above-ground biomass using terrestrial laser scanning. *Methods Ecol. Evol.* 6 (2), 198–208.
- Chang, C.-C., Lin, C.-J., 2011. LIBSVM : a library for support vector machines. *ACM Trans. Intell. Syst. Technol.* 2 (27), 27, 1–27.
- Chiu, C., Thelwell, M., Senior, T., 2019. Comparison of depth cameras for three-dimensional reconstruction in medicine. *Proc. Instit. Mech. Eng. H-J. Eng. Med.* 233 (9), 938–947.
- Dey, D., Mummert, L., Sukthankar, R., 2012. Classification of plant structures from uncalibrated image sequences. *IEEE*.
- Díaz, C.A., et al., 2018. Grapevine buds detection and localization in 3D space based on Structure from Motion and 2D image classification. *Comput. Ind.* 99, 303–312.
- Gan, H., et al., 2018. Immature green citrus fruit detection using color and thermal images. *Comput. Electron. Agric.* 152, 117–125.
- Gangadharan, S., Burks, T.F., Schueler, J.K., 2019. A comparison of approaches for citrus canopy profile generation using ultrasonic and Leddar® sensors. *Comput. Electron. Agric.* 156, 71–83.

- Gené-Mola, J., et al., 2019. Multi-modal deep learning for Fuji apple detection using RGB-D cameras and their radiometric capabilities. *Comput. Electron. Agric.* 162, 689–698.
- Gongal, A., et al., 2016. Apple crop-load estimation with over-the-row machine vision system. *Comput. Electron. Agric.* 120, 26–35.
- Hu, H., et al., 2018. Stretchable ultrasonic transducer arrays for three-dimensional imaging on complex surfaces. *Sci. Adv.* 4 (3) p. eaar3979.
- Jamayet, N.B., et al., 2018. A fast and improved method of rapid prototyping for ear prosthesis using portable 3D laser scanner. *J. Plast. Reconstr. Aesthetic Surg.* 71 (6), 946–953.
- Jay, S., et al., 2015. In-field crop row phenotyping from 3D modeling performed using Structure from Motion. *Comput. Electron. Agric.* 110, 70–77.
- Kleppe, A.L., Egeland, O., 2018. A curvature-based descriptor for point cloud alignment using conformal geometric algebra. *Adv. Appl. Clifford Algebr.* 28 (2).
- Krishna, M.S., et al., 2019. Semi-automatic extraction of liana stems from terrestrial LiDAR point clouds of tropical rainforests. *ISPRS J. Photogramm. Remote. Sens.* 154, 114–126.
- Lei, X., Ouyang, H., Xu, L., 2019. Mature pomegranate recognition methods in natural environments using machine vision. *Ciencia Rural* 49 (9).
- Li, B., et al., 2018. Detection of green apples in natural scenes based on saliency theory and Gaussian curve fitting. *Int. J. Agric. Biol. Eng.* 11 (1), 192–198.
- Li, M., Rottensteiner, F., Heipke, C., 2019. Modelling of buildings from aerial LiDAR point clouds using TINs and label maps. *ISPRS J. Photogramm. Remote. Sens.* 154, 127–138.
- Lin, G., et al., 2019. Guava detection and pose estimation using a low-cost RGB-D sensor in the field. *Sensors (Basel)* 19 (2), 428.
- Linker, R., 2017. A procedure for estimating the number of green mature apples in night-time orchard images using light distribution and its application to yield estimation. *Precis. Agric.* 18 (1), 59–75.
- Liu, T., et al., 2019a. Identifying immature and mature pomelo fruit in trees by elliptical model fitting in the Cr-Cb color space. *Precis. Agric.* 20 (1), 138–156.
- Liu, Xiaoyang, Zhao, Dean, Jia, Weikuan, Ji, Wei, Sun, Yueping, 2019b. A detection method for apple fruit based on color and shape features. *IEEE Access* 7, 67923–67933.
- Lu, J., et al., 2018. Immature citrus fruit detection based on local binary pattern feature and hierarchical contour analysis. *Biosyst. Eng.* 171, 78–90.
- Lu, Jidong, Wang, Fan, Xu, Liming, Ma, Zhenghua, Yang, Biao, 2019a. A segmentation method of bagged green apple image. *Sci. Hortic.* 246, 411–417.
- Lu, Jidong, Ni, Huanmin, Wang, Qi, Yang, Biao, Xu, Liming, 2019b. A segmentation method of red apple image. *Sci. Hortic.* 256, p. 108615.
- Madec, S., et al., 2017. High-throughput phenotyping of plant height: comparing unmanned aerial vehicles and ground LiDAR estimates. *Front. Plant Sci.* 8.
- Mohammadi, V., Kheiraliipour, K., Ghasemi-Varnamkhasti, M., 2015. Detecting maturity of persimmon fruit based on image processing technique. *Sci. Hortic.* 184, 123–128.
- Niu, L., et al., 2017. Extracting the symmetry axes of partially occluded single apples in natural scene using convex hull theory and shape context algorithm. *Multimed. Tools Appl.* 76 (12), 14075–14089.
- Nyarko, E.K., et al., 2018. A nearest neighbor approach for fruit recognition in RGB-D images based on detection of convex surfaces. *Expert Syst. Appl.* 114, 454–466.
- Park, C.S., et al., 2018. Application of 3D laser scanner to forensic engineering. *J. Forensic Sci.* 63 (3), 930–934.
- Pearse, G.D., et al., 2019. Comparison of models describing forest inventory attributes using standard and voxel-based lidar predictors across a range of pulse densities. *Int. J. Appl. Earth Obs. Geoinf.* 78, 341–351.
- Pomerleau, F., Colas, F., Siegwart, R., Magnenat, S., 2013. Comparing ICP variants on real-world data sets. *Auton. Robots Vol. 34 (Issue 3, April)*, 133–148.
- Qiu, Q., et al., 2019. Field-based high-throughput phenotyping for maize plant using 3D LiDAR point cloud generated with a “Phenomobile”. *Front. Plant Sci.* 10.
- Ramos, P.J., Avendaño, J., Prieto, F.A., 2018. Measurement of the ripening rate on coffee branch by using 3D images in outdoor environments. *Comput. Ind.* 99, 83–95.
- Rosell, J.R., Sanz, R., 2012. A review of methods and applications of the geometric characterization of tree crops in agricultural activities. *Comput. Electron. Agric.* 81, 124–141.
- Stein, M., Bargoti, S., Underwood, J., 2016. Image based mango fruit detection, localisation and yield estimation using multiple view geometry. *Sensors* 16 (11), p. 1915.
- Tan, K., et al., 2018. Recognising blueberry fruit of different maturity using histogram oriented gradients and colour features in outdoor scenes. *Biosyst. Eng.* 176, 59–72.
- Tao, Yongting, Zhou, Jun, Zhou, J., 2017. Automatic apple recognition based on the fusion of color and 3D feature for robotic fruit picking. *Comput. Electron. Agric.* 142, 388–396.
- Tu, S., et al., 2018. Detection of passion fruit and maturity classification using Red-Green-Blue Depth images. *Biosyst. Eng.* 175, 156–167.
- Wang, Z., Walsh, K., Verma, B., 2017. On-tree mango fruit size estimation using RGB-D images. *Sensors* 17 (12), 2738.
- Westling, F., Underwood, J., Örn, S., 2018. Light interception modelling using unstructured LiDAR data in avocado orchards. *Comput. Electron. Agric.* 153, 177–187.
- Wu, J., et al., 2019. Automatic recognition of ripening tomatoes by combining multi-feature fusion with a Bi-layer classification strategy for harvesting robots. *Sensors* 19 (3), 612.
- Xu, L., Lv, J., 2018. Recognition method for apple fruit based on SUSAN and PCNN. *Multimed. Tools Appl.* 77 (6), 7205–7219.
- Yamamoto, K., et al., 2014. On plant detection of intact tomato fruit using image analysis and machine learning methods. *Sensors* 14 (7), 12191–12206.
- Yan, W.Y., Shaker, A., El-Ashmawy, N., 2015. Urban land cover classification using airborne LiDAR data: a review. *Remote Sens. Environ.* 158, 295–310.
- Yang, S., et al., 2018. A dual-platform laser scanner for 3D reconstruction of dental pieces. *Engineering* 4 (6), 796–805.
- Zhou, J., et al., 2019. Automated segmentation of soybean plants from 3D point cloud using machine learning. *Comput. Electron. Agric.* 162, 143–153.